Inactivation of Smad4 Accelerates Kras^{G12D}-Mediated Pancreatic Neoplasia

Kyoko Kojima,[1] Selwyn M. Vickers,[3] N. Volkan Adsay,[4] Nirag C. Jhala,[2] Hyung-Gyoon Kim,[1] Trenton R. Schoeb,[2] William E. Grizzle,[2] and Christopher A. Klug[1]

Departments of [1]Microbiology and [2]Pathology, The University of Alabama at Birmingham, Birmingham, Alabama; [3]Department of Surgery, University of Minnesota, Minneapolis, Minnesota; and [4]Department of Pathology, Wayne State University, Detroit, Michigan

Abstract

Pancreatic ductal adenocarcinoma (PDAC) is one of the most fatal human malignancies, with an overall 5-year survival rate of <5%. Genetic analysis of PDAC patient samples has shown that specific disease-associated mutations are correlated with histologically defined stages of neoplastic progression in the ductal epithelium. Activating mutations in *KRAS* are almost uniformly present in early-stage disease, with subsequent inactivating mutations in *p16^{INK4A}*, *p53*, and *SMAD4* occurring in more advanced lesions. In this study, we have tested whether the loss of Smad4 would cooperate with an activating *Kras^{G12D}* mutation to promote progression to PDAC using the *Pdx1-Cre* transgenic system to activate *Kras^{G12D}* and delete *Smad4* in all pancreatic lineages including the ductal epithelium. Analysis of double-mutant mice showed that loss of Smad4 significantly accelerated the progression of pancreatic intraepithelial neoplasias (mPanIN) and promoted a high incidence of intraductal papillary mucinous neoplasia and active fibrosis compared with *Pdx1-Cre;Kras^{G12D}* or *Pdx1-Cre;Smad4$^{lox/lox}$* mice. Occasionally, double-mutant mice progressed to locally invasive PDAC with little evidence of metastases by 6 months of age and without the detectable loss of p53 or p16^{Ink4A} expression or function. The loss of Smad4 only seemed to promote disease progression in the presence of the activated *Kras^{G12D}* allele because we observed no abnormal pathology within the pancreata of 23 *Pdx1-Cre;Smad4$^{lox/lox}$* animals that were analyzed up to 8 months of age. This indicates that Smad4 is dispensable for normal pancreatic development but is critical for at least partial suppression of multiple Kras^{G12D}-dependent disease-associated phenotypes. [Cancer Res 2007;67(17):8121–30]

Introduction

Infiltrating pancreatic ductal adenocarcinoma (PDAC) is the fourth leading cause of cancer death in the United States. It is almost uniformly fatal, with an overall 5-year survival rate of <5% (1, 2). The extremely poor prognosis associated with PDAC is primarily due to the advanced stage of disease at the time of clinical diagnosis and the refractory nature of PDAC to conventional chemotherapy and radiotherapy regimens.

Preinvasive neoplasias affecting the pancreatic ductal epithelium have been grouped into three major pathologic categories that include pancreatic intraepithelial neoplasias (PanIN), which are primarily observed in the small ducts, intraductal papillary mucinous neoplasms (IPMN), which occur in the main pancreatic duct or in branch ducts, and mucinous cystic neoplasms, where cystic lesions are lined by a mucin-producing, tall columnar epithelium with an associated ovarian-type stroma.

Histologic and molecular genetic characterization of ductal lesions before invasive PDAC has led to the development of a staged progression model wherein the presence of specific disease-associated mutations is correlated with defined histologic abnormalities in the ductal epithelium (3, 4). Neoplasias representing PanIN range from PanIN-1A and PanIN-1B to PanIN-2 and PanIN-3, with each stage showing increased cellular and nuclear atypia (5, 6). PanIN-3 is frequently found in association with invasive PDAC and likely represents a precursor lesion to invasive disease.

A number of mutations have been associated with specific PanIN stages, including the activation of the *KRAS2* and *HER-2/NEU* genes and the loss of the tumor suppressor proteins CDKN2A/p16^{INK4A}, p53, DPC4/SMAD4, and BRCA2 (7). The presence of an activating mutation in the *KRAS2* locus was detected in ~40% of early PanIN-1A and PanIN-1B lesions and is found in virtually 100% of advanced PDAC cases (8–12). Analysis of mice where a *Pdx1-Cre* transgene was used to activate expression of a constitutively active allele of *Kras* (*Kras^{G12D}*) in the ductal epithelium showed the full spectrum of preinvasive PanIN-like lesions (mPanIN), which supports the model that *Kras* activation is a critical initiating step in progression to PDAC (13, 14). Although loss of p16^{INK4A} tumor suppressor expression can be detected in PanIN-1A and PanIN-1B lesions, it is more frequently associated with PanIN-2, wherein the ductal epithelium exhibits nuclear atypia and papillary architecture (15). In invasive PDAC, more than 90% of cases show loss of p16^{INK4A} function (12, 16–19). In mice, loss of either p16^{Ink4A} or p53 in conjunction with constitutive Kras activity promotes progression to PDAC, which indicates that both the retinoblastoma (Rb) and p53 pathways are involved in suppression of PDAC progression (20, 21). However, the observation that p53 remains intact in a *Pdx1-Cre;Kras$^{G12D/+}$;p16$^{Ink4A-/-}$* genetic background that progresses to PDAC and that p16^{Ink4A} remains intact in *Pdx1-Cre;Kras^{G12D};p53$^{-/-}$* ductal epithelia with PDAC indicates that inactivation of both pathways may not be necessary for fully penetrant disease in the mouse model.

Finally, inactivating mutations in the gene encoding the downstream transforming growth factor β (TGF-β) effector protein, *d*eleted in *p*ancreatic *c*ancer 4 (DPC4/SMAD4/MADH4), have been found in association with late stages of PDAC progression when there is evidence of carcinoma *in situ* and invasive disease in ~55% of PDAC cases (22, 23). The loss of DPC4/SMAD4 has also been associated with familial juvenile polyposis (24) and

Note: Supplementary data for this article are available at Cancer Research Online (http://cancerres.aacrjournals.org/).

Requests for reprints: Christopher A. Klug, The University of Alabama at Birmingham, Shelby Room 510, 1825 University Avenue, Birmingham, AL 35294. Phone: 205-934-1424; E-mail: chrisk@uab.edu.

doi:10.1158/0008-5472.CAN-06-4167

with ~15% of colorectal tumors (25). In mice, haploinsufficiency of Smad4 was sufficient to initiate gastric polyp formation and progression to invasive carcinoma that was associated with loss of the wild-type *Smad4* allele in older animals (26). In a number of human PDAC cell lines that lack SMAD4, TGFβ signaling through the receptor-associated SMADs, SMAD2 and SMAD3, seems to be intact in that both proteins are serine phosphorylated and localized to the nucleus (27, 28). It has been proposed that the loss of SMAD4 may abrogate TGFβ-induced cell cycle arrest but maintain TGFβ-dependent, SMAD4-independent signaling pathways that function in tumor promotion (29).

Mutational analyses of IPMN samples have revealed similar genetic abnormalities to what has been observed in PanIN lesions, with a high incidence of activating *KRAS* mutations and loss of p16 and p53 expression (30–32). Loss of SMAD4 is not typically found in association with IPMN (32, 33).

In this study, we have tested whether the loss of Smad4 would cooperate with an activating $Kras^{G12D}$ mutation to promote progression to PDAC using the *Pdx1-Cre* transgenic system (34, 35). Analysis of double-mutant mice showed that loss of Smad4 significantly accelerated the progression of mPanIN lesions, the loss of acinar tissue, and the appearance of active fibrosis compared with single-mutant $Pdx1\text{-}Cre;Kras^{G12D/+}$ or $Pdx1\text{-}Cre;Smad4^{lox/lox}$ mice. $Pdx1\text{-}Cre;Smad4^{lox/lox}$ mice showed no gross histologic abnormalities in the pancreas up to 8 months of age. A high frequency of double-mutant mice (14 of 16) also exhibited IPMN-like lesions of the gastric type and displayed duct ectasia with an associated pancreatitis. Lesions resembling mucinous cystic neoplasm were not observed in any of the animals and there was no evidence of ovarian-type stroma as determined by histologic examination and by negative staining for progesterone and estrogen receptor. These results indicate that, in conjunction with $Kras^{G12D}$, the loss of Smad4 may stimulate PDAC progression through multiple factors including accelerated fibrosis, enhanced acinar cell loss, and more rapid promotion of neoplastic changes resembling mPanIN and IPMN within the ductal epithelium.

Materials and Methods

Mouse strains. The *Pdx1-Cre* transgenic strain originally generated on an ICR background was kindly provided by Doug Melton (35) and was backcrossed to C57BL/6 for four generations. The $LSL\text{-}Kras^{G12D/+}$ knock-in strain on a C57BL/6/129SvJae background was purchased from the Mouse Models of Human Cancer Consortium (National Cancer Institute-Frederick) and was backcrossed to C57BL/6 for five generations. The floxed *Smad4* strain on a C57BL/6 background was a kind gift from Chu-Xia Deng (36). The genotypes $Pdx1\text{-}Cre;Smad4^{lox/+}$ and $Kras^{G12D/+};Smad4^{flox/+}$ were intercrossed to generate double-mutant mice ($Pdx1\text{-}Cre;Kras^{G12D/+};Smad4^{lox/lox}$). Genomic and recombination screens were done by PCR (primer sequences are given in Supplementary Methods).

Histology and immunohistochemistry. Tissues were fixed either in 70% ethanol/10% neutral buffered formalin overnight or in 4% paraformaldehyde in PBS for 4 h, and embedded in paraffin. Routine H&E staining was done by the Tissue Procurement Core Facility at University of Alabama at Birmingham. For immunohistochemistry, 4-μm sections were deparaffinized in xylene and rehydrated in ethanol. Heat-induced epitope retrieval was done on all slides in Tris-EDTA buffer (10 mmol/L Tris base, 1 mmol/L EDTA solution, 0.05% Tween 20, pH 9.0) using a Russell Hobbs Pressure Cooker (Fisher Scientific) at high setting for 10 min. Slides were incubated with 3% hydrogen peroxide to block endogenous peroxidase activity and then incubated with avidin/biotin blocking reagent (Vector Laboratories). Tissue sections were blocked at room temperature for 1 h using 3% normal goat serum, 1.5% normal horse serum, 2% normal rabbit serum, or Vector M.O.M. Basic Kit (Vector Laboratories) according to the manufacturer's instructions. Primary staining was done at room temperature for 1 h, followed by 20-min incubation with biotinylated secondary antibodies. Vectastain Elite ABC Kit (Vector Laboratories), which contains SA-peroxidase, was used for biotin labeling. DAB Substrate Kit (Vector Laboratories) was used for visualization of peroxidase activity. Hematoxylin counterstaining was then done. Slides were dehydrated in ethanols and xylene and mounted with VectaMount permanent mounting medium (Vector Laboratories). The primary antibodies used were Smad4 (B-8, Santa Cruz Biotechnology), pSmad2 (Abcam), CK19 (BA17, DakoCytomation), Ki-67 (Abcam and Novus Biologicals), Muc1 (Abcam), Muc2 (H-300, Santa Cruz Biotechnology), PR (Abcam), and ER (Abcam). Secondary antibodies were biotinylated goat anti-rabbit immunoglobulin G (IgG; Vector Laboratories), biotinylated horse anti-goat IgG (Vector Laboratories), and biotinylated anti-mouse IgG from Vector M.O.M. Basic Kit following the manufacturer's instruction. For Alcian blue staining, 4-μm sections were deparaffinized and rehydrated. Slides were stained with Alcian blue solution (1-g Alcian blue in 100-mL 3% glacial acetic acid, pH 2.5) for 30 min at room temperature. Counterstaining with 0.1% nuclear fast red solution (0.1-g nuclear fast red and 5-g ammonium sulfate in 100-mL dH_2O) was done for 5 min. Slides were dehydrated and mounted.

Western blotting. Primary ductal cell lines (see Supplementary Methods) were harvested and lysed (20 mmol/L HEPES, 2 mmol/L EDTA, 250 mmol/L NaCl, 0.1% NP_4O, 2 μg/mL aprotinin, 2 μg/mL leupeptin, 2 μg/mL pepstatin, 0.5 mg/mL benzamidine, 1 mmol/L phenylmethylsulfonyl fluoride) for 10 min on ice. Protein concentration was measured with Quick Start Bradford Protein Assay (Bio-Rad Laboratories). Protein (5 or 50 μg/lane) was resolved on 12% acrylamide gels and transferred to polyvinylidene difluoride membranes. Membranes were blocked with 3% Carnation nonfat dry milk in PBS-0.5% Tween 20 and sequentially incubated with primary and secondary antibodies. Protein detection was done with SuperSignal West Femto Maximum Sensitivity Substrate kit (Pierce Biotech). The primary antibodies used were Smad4 (B-8, Santa Cruz Biotechnology), p15 (Cell Signaling), p16 (M-156, Santa Cruz Biotechnology), pRb (Cell Signaling), p53 (FL-393, Santa Cruz Biotechnology), p21 (SX118, BD PharMingen), CK19 (BA17, DakoCytomation), and β-actin (A5441, Sigma-Aldrich). The secondary antibodies used were goat anti-mouse IgG-horseradish peroxidase (HRP) and goat anti-rabbit IgG-HRP from SuperSignal West Femto Maximum Sensitivity Substrate kit. Positive controls were 3T3 lysates (for p16, p15, p21, and Smad4), purified phospho-Rb-C (for Rb), and WR19L cell lysate (for p53). For Ras activity assay, pancreatic tissues were digested with 4 mg/mL each of dispaseII/collagenase for 20 min at 37°C. Digested samples were then lysed in Mg^{2+} lysis buffer (Ras Activation Assay kit, Upstate Cell Signaling Solutions) and 1 mg of each lysate was used to measure Ras activity.

Results

Loss of Smad4 accelerates development of mPanIN lesions induced by oncogenic $Kras^{G12D}$. To determine whether the loss of Smad4 would cooperate with a constitutively active allele of *Kras* to promote progression of PDAC, we generated F1 progeny by crossing $Pdx1\text{-}Cre;Smad4^{lox/+}$ and $Kras^{G12D/+};Smad4^{flox/+}$ animals (Fig. 1*A*). Activation of the inducible $Kras^{G12D}$ allele occurs by Cre-mediated deletion of transcriptional and translational stop sequences that were inserted upstream of the first coding exon of the *Kras* locus that also contained a knocked-in G12D mutation (13, 37). Genotyping of animals was done by PCR, whereas expression of activated $Kras^{G12D}$ within pancreatic tissue was assessed using a pull-down assay to quantify the level of Ras-GTP (Fig. 1*A*). Deletion of floxed sequences within the *Smad4* locus results in the loss of exon 8 and generates a null *Smad4* allele in all endocrine and exocrine cells due to expression of the *Pdx1-Cre* transgene in pancreatic progenitor cells (Fig. 1*A*; refs. 34–36). Double-mutant animals ($Pdx1\text{-}Cre;Kras^{G12D/+};Smad4^{lox/lox}$) were

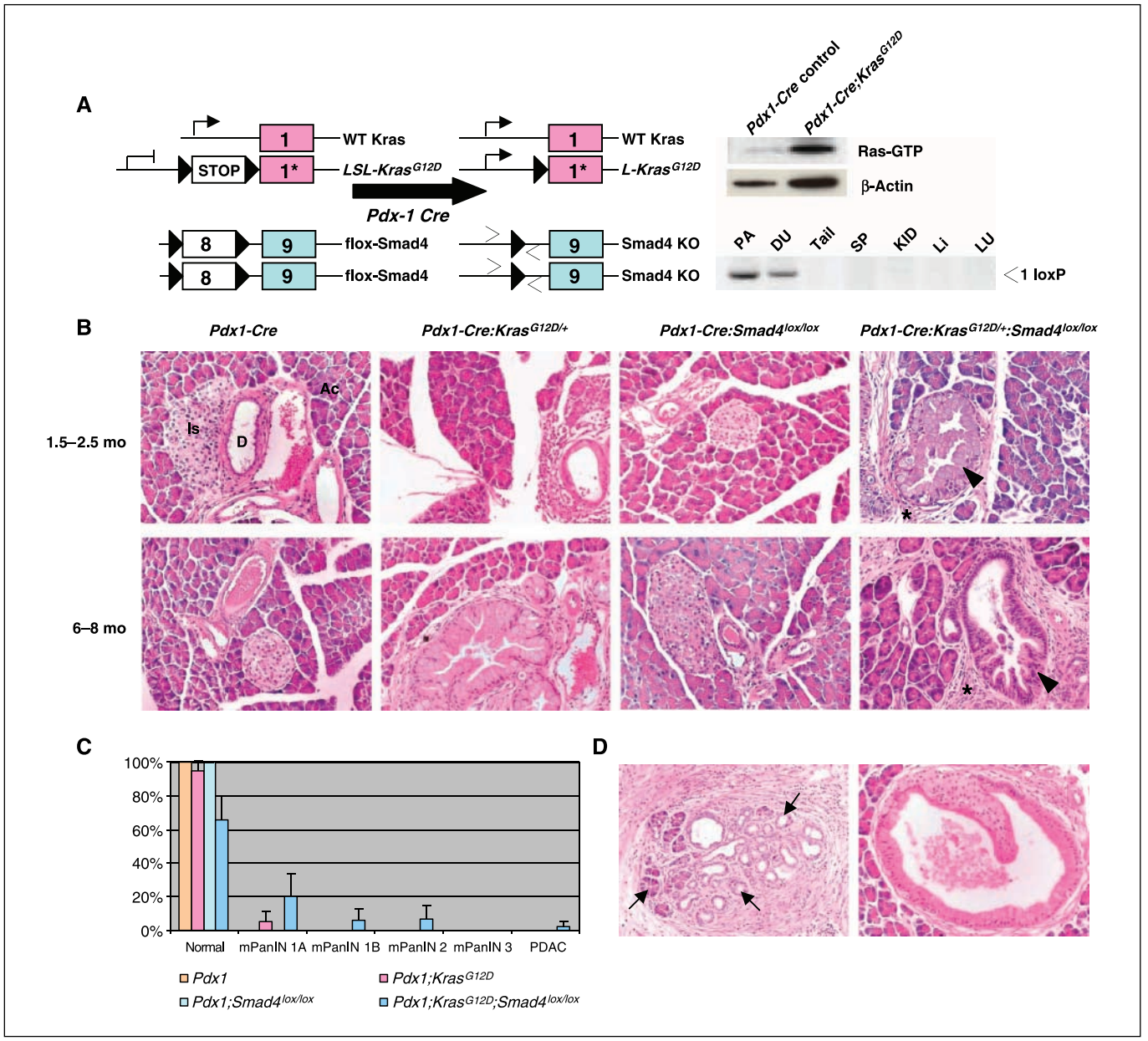

Figure 1. Generation of *Pdx1-Cre;Kras$^{G12D/+}$;Smad4$^{lox/lox}$* mice. *A, Pdx1-Cre*–mediated conditional expression of Kras^{G12D} and deletion of *Smad4. Arrows,* PCR primers for recombination screening. Ras activity was measured using a pull-down assay and Western blot to quantify GTP-bound RAS. Deletion of *Smad4* in the indicated tissues of a 6-wk-old *Pdx1-Cre;Kras$^{G12D/+}$;Smad4$^{lox/lox}$* animal was assessed by PCR (*PA,* pancreas; *DU,* duodenum; *SP,* spleen; *KID,* kidney; *Li,* liver; *LU,* lung). *B,* H&E staining of representative *Pdx1-Cre* control and single- and double-mutant animals at 1.5 to 2.5 mo and at 6 to 8 mo of age (*D,* duct; *Ac,* acinar tissue; *Is,* islet; all images at ×200). *Pdx1-Cre* (n = 5 at 1.5–2.5 mo, n = 7 at 6–8 mo), *Pdx1-Cre;Smad4$^{lox/lox}$* (n = 3 at 1.5–2.5 mo, n = 10 at 6–8 mo), *Pdx1-Cre;Kras$^{G12D/+}$* mice (n = 4 at 1.5–2.5 mo, n = 5 at 6–8 mo), and *Pdx1-Cre;Kras$^{G12D/+}$;Smad4$^{lox/lox}$* mice (n = 4 at 1.5–2.5 mo, n = 5 at 6–8 mo). *Top right, arrowhead,* duct with mPanIN-1A lesion at 6 wks of age; *bottom right, arrowhead,* a higher-grade mPanIN-2 lesion at 33 wks of age. *Asterisks,* active fibrosis. *C,* accelerated progression of histologically advanced mPanIN in *Pdx1-Cre;Kras$^{G12D/+}$;Smad4$^{lox/lox}$* mice at 1.5 to 2.5 mo of age. *Columns,* percentages of normal and mPanIN by grade in four genotypes; *bars,* SE. A minimum of 50 total ducts counted from at least three independent animals were typed for each genotype [*Pdx1-Cre* (n = 5), *Pdx1-Cre;Kras$^{G12D/+}$* (n = 4), *Pdx1-Cre;Smad4$^{lox/lox}$* (n = 3), and *Pdx1-Cre;Kras$^{G12D/+}$;Smad4$^{lox/lox}$* (n = 4)]. *D,* focal acinar-ductal metaplasia (*left*; 33-wk-old animal) and ductulo-insular complex (*right*; 9-wk-old animal) in *Pdx1-Cre;Kras$^{G12D/+}$;Smad4$^{lox/lox}$* mice (×200).

generated at the expected Mendelian frequencies, indicating that Pdx1-Cre–mediated inactivation of Smad4 was not lethal.

Histopathologic analysis of pancreatic tissue within single-mutant (*Kras$^{G12D/+}$* or *Smad4$^{lox/lox}$* alone) or double-mutant animals at both early (1.5–2.5 months) and late (6–8 months) time points showed normal exocrine glandular components and islets in *Pdx1-Cre* control (n = 5 at 1.5–2.5 months, n = 7 at 6–8 months) and in *Pdx1-Cre;Smad4$^{lox/lox}$* animals (n = 3 at 1.5–2.5 months, n = 10 at 6–8 months; Fig. 1*B*). *Pdx1-Cre;Kras$^{G12D/+}$* mice (n = 4 at 1.5–2.5 months, n = 5 at 6–8 months) had low frequencies of low-grade PanIN-like lesions (mPanIN) at 1.5 to 2.5 months and more advanced preinvasive lesions and focal acinar-ductal metaplasia at later time points as previously reported (Fig. 1*B*; refs. 13, 14). Analysis of *Pdx1-Cre;Kras$^{G12D/+}$;Smad4$^{lox/lox}$* mice showed significantly accelerated progression of more advanced mPanIN (mPanIN-2) and the appearance of active fibrosis as

compared with age-matched *Pdx1-Cre;Kras$^{G12D/+}$* mice (Fig. 1*B* and *C*). Only 1 of 17 double-mutant animals lived beyond 33 weeks of age, which limited comparative analyses beyond this point. Due to the near-complete loss of acinar tissue, which was mediated in part through acinar-ductal metaplasia (Fig. 1*D, left*), accurate assessment of mPanIN was often difficult in older animals and was typed in younger double-mutant animals with less severe acinar loss. Low-power examination of H&E-stained double-mutant pancreata used for Fig. 1*C* is shown in Supplementary Fig. S1; mouse nos. 490, 523, and 506, with mouse no. 484 not being used for analysis due to extensive acinar cell loss. In addition, *Pdx1-Cre;Kras$^{G12D/+}$;Smad4$^{lox/lox}$* mice commonly exhibited ductulo-insular complex involvement in both young and older animals (Table 1; Fig. 1*D, right*).

***Pdx1-Cre;Kras$^{G12D/+}$;Smad4$^{lox/lox}$* mice progress to locally invasive PDAC with infrequent instances of metastases.** Further characterization of older *Pdx1-Cre;Kras$^{G12D/+}$;Smad4$^{lox/lox}$* mice showed that animals between 23 and 33 weeks of age exhibited progression to either locally invasive PDAC without metastases (Fig. 2*A–C*, three of five cases) or, more rarely, to adenocarcinoma with sarcomatoid features that had metastasized to the liver (Fig. 2*D* and *E*; Table 1; mouse no. 239). One younger animal also exhibited invasive, moderately differentiated adenosquamous carcinoma (Fig. 2*F*; Table 1, mouse no. 484). All older *Pdx1-Cre;Kras$^{G12D/+}$;Smad4$^{lox/lox}$* mice had very limited normal endocrine or exocrine tissue that remained, and the overall size of the pancreas was significantly expanded (Table 1; Supplementary Fig. S1).

***Pdx1-Cre;Kras$^{G12D/+}$;Smad4$^{lox/lox}$* mice exhibit IPMN-like lesions with duct ectasia and chronic pancreatitis.** In the majority of both young and older *Pdx1-Cre;Kras$^{G12D/+}$;Smad4$^{lox/lox}$* mice (14 of 16 moribund animals, Table 1), we observed cystic lesions resembling IPMN of the gastric/foveolar subtype that occurred with or without evidence of papillae (Fig. 2*G–L*; refs. 6, 38, 39). In most cases, the IPMN was an intraductal papillary mucinous adenoma (IPMA) that involved the branch ducts, which presented without significant architectural atypia and without papillae formation (Fig. 2*G*). IPMA was often accompanied by pancreatitis with duct ectasia and the occasional presence of inflammatory cells within the ducts (Supplementary Fig. S1, mouse no. 456, and data not shown). In cases of IPMN with papillae formation (Fig. 2*H–L*), we observed rare instances where fibrovascular cores contained endocrine cells (Fig. 2*H* and *I*). A papilla composed of acinar cells was also noted in one case (Fig. 2*J*). Mucinous ducts stained positive for Muc1 and were Muc2 negative (Supplementary Fig. S2*A*). The surrounding stroma lacked expression of both progesterone and estrogen receptor (Supplementary Fig. S2*B*) and did not exhibit "wavy" appearing nuclei, which are a characteristic of stroma associated with mucinous cystic neoplasm in humans. The presence of cystic lesions was also evident on gross examination of the pancreas, where large nodules were clearly evident within the expanded parenchyma (Supplementary Fig. S3). We did not observe cystic lesions in *Pdx1-Cre;Smad4$^{lox/lox}$* animals but did note focal IPMA in two of six older *Pdx1-Cre;Kras$^{G12D/+}$* mice that was not associated with the loss of Smad4 based on immunohistochemical staining (ages 24 and 30 weeks; Fig. 2*M–P* and data not shown). Pancreata from these mice also showed ductulo-insular complex involvement (Fig. 2*Q* and *R*), indicating that these structures may be derived from Smad4-independent changes occurring downstream of Kras^{G12D} expression.

Immunohistochemical characterization of *Pdx1-Cre;-Kras$^{G12D/+}$;Smad4$^{lox/lox}$* mice. Further characterization of *Pdx1-Cre;Kras$^{G12D/+}$;Smad4$^{lox/lox}$* and *Pdx1-Cre;Smad4$^{lox/lox}$* animals at 33 weeks of age showed that Smad4 expression was lost in ductal epithelial cells (Fig. 3, *top row, arrowheads*) and in acinar cells, whereas high-level expression remained evident in the stroma (*two right columns, arrows*). Because Pdx1 is expressed in pancreatic progenitor cells during development, Pdx1-Cre would not be expected to delete Smad4 within the stromal compartment in *Pdx1-Cre;Smad4$^{lox/lox}$* mice. Ductal epithelia that lacked Smad4 showed nuclear phospho-Smad2 expression, which indicates that certain arms of the TGFβ signaling pathway remain intact in the absence of Smad4 (Fig. 3). Ductal lesions were composed of epithelial cells, as determined by CK19 positivity (see Fig. 3, *arrowheads*) and expressed mucin based on Alcian blue staining (Fig. 3). Ki-67 staining of the ductal epithelium showed that Kras^{G12D} expression enhanced ductal proliferation ~2-fold in histologically normal ducts (as compared with *Pdx1-Cre* control ducts) and was significantly increased in high-grade mPanIN lesions as previously described (Supplementary Table S1; Supplementary Fig. S4; ref. 13). The loss of Smad4 had a modest, but statistically significant, effect in promotion of Kras^{G12D}-associated ductal proliferation in early-stage mPanIN-1A lesions ($P < 0.05$; Table 2). Higher frequencies of proliferating ductal cells in more advanced mPanIN lacking Smad4 were noted but were not statistically significant. There was no increase in Ki-67 staining in the apparently normal ductal epithelium of *Pdx1-Cre;Smad4$^{lox/lox}$* animals compared with *Pdx1-Cre* control mice.

Loss of Smad4 in the context of Kras^{G12D} promotes progression to PDAC without the loss of p16^{Ink4A} or p53. Because human PDAC is associated with the loss of the p16^{INK4A} and p53 tumor suppressors in ~90% and 75% of cases, respectively, we analyzed four independent pancreatic ductal epithelial cell lines that were clonally derived from each of two moribund *Pdx1-Cre;Kras$^{G12D/+}$;Smad4$^{lox/lox}$* mice to determine if histopathologic progression might be due to the loss of either p16^{Ink4A} and/or p53 function (see Supplementary Fig. S5 for representative morphology of murine ductal cell lines compared with a human ductal epithelial cell line and for CK19 expression). Western blot analysis using an equivalent amount of protein from a pancreatic cell line derived from a *Pdx1-Cre;Kras$^{G12D/+}$* animal (Fig. 4, *Ras*) or from representative early-passage cell lines clonally isolated from *Pdx1-Cre;Kras$^{G12D/+}$;Smad4$^{lox/lox}$* mice (mouse nos. 162 and 537, Table 1) showed that both p53 and the p53 target gene, p21/Waf1/Cip1, were highly induced by γ-irradiation (10 Gy using a cobalt source). Sequencing of a PCR product amplified from the p53 locus also revealed that no point mutations had occurred within the p53 coding sequences (data not shown). These results suggest that the p53 signaling pathway remained intact in the presence of the *Kras^{G12D}* and *Smad4$^{lox/lox}$* mutations. Because p16^{Ink4A} is known to regulate cdk4 and cdk6 phosphorylation of the Rb protein, we analyzed for expression of both p16^{Ink4A} and phosphorylated Rb (pRb) in *Kras^{G12D};Smad4$^{lox/lox}$* mutant cells. Figure 4 shows that both phosphorylated forms of Rb were present in *Kras^{G12D};Smad4$^{lox/lox}$* mutant cells as was p16^{Ink4A}. These results indicate that significant acceleration of pancreatic neoplasia in *Pdx1-Cre;Kras$^{G12D/+}$;Smad4$^{lox/lox}$* mice can occur in the presence of p16^{Ink4A} and p53. Previous studies have shown that TGFβ signaling via a Smad4-dependent pathway can induce transcription of both p15^{Ink4B} and p21/Waf1 (40–42); thus, we tested whether p15^{Ink4B} expression was affected in Smad4-deficient cells. Western blot

Table 1. Characterization of moribund *Pdx1-Cre;Kras$^{G12D/+}$;Smad4$^{lox/lox}$* mice

ID	Age (wk)	Weight loss*	Bloody ascites	% Abnormal PA†	PA	DU	ST
484	6	N	Y	100	IPMN-like; invasive mPDAC; adenosquamous carcinoma	Polypoid obstruction	Normal
490	6	N	N	40	Duct ectasia; invasive mPDAC	Early polypoid lesions	Polypoid lesions; squamous cell carcinoma from esophagus
523	6	Y	N	50	Ductulo-insular units; duct ectasia	Early polypoid lesions	Early squamous cell carcinoma from esophagus
506	9	N	N	30	Ductulo-insular units; neutrophilic ducts; mPanIN 2; IPMN-like; focal mPDAC	N/A	Normal
482	11	Y	N	30	Ductulo-insular units; mPanIN 2; IPMN-like	Early polypoid lesions	Early polypoid lesions
224	12	Y	N	20	Duct ectasia; mPanIN 1B; IPMN-like	Normal	Squamous cell carcinoma from esophagus
456	12	N	N	90	Chronic pancreatitis; neutrophilic ducts; mPanIN 2; IPMN-like; focal mPDAC	Early polypoid lesions	Early polypoid lesions
537	14	N	N	70	Chronic pancreatitis; mPanIN 1B; IPMN-like	Early polypoid lesions	Normal
181	15	Y	N	50	mPanIN 1B; IPMN-like	Polyp; focal carcinoma *in situ*	Early polypoid lesions
399	15	N	N	30	mPanIN 1B; IPMN-like	Normal	Normal
62	18	Y	Y	60	Duct ectasia; chronic pancreatitis; neutrophilic ducts; mPanIN 2; IPMN-like	Polypoid obstruction	Squamous cell carcinoma from esophagus
239	23	N	Y	95	IPMN-like; carcinosarcoma	N/A	Polypoid lesions
493	24	N	N	85	Chronic pancreatitis; IPMN-like; focal mPDAC	Polyp; focal carcinoma *in situ*	Normal
7	25	N	Y	70	Neutrophilic ducts; mPanIN 3; IPMN-like; microinvasive mPDAC	Polypoid obstruction; carcinoma *in situ*	Normal
465	27	N	N	60	Duct ectasia; chronic pancreatitis; neutrophilic ducts; mPanIN 2; IPMN-like	Early polypoid lesions	Normal
162	33	N	N	98	Duct ectasia; chronic pancreatitis; mPanIN 3; IPMN-like; focal mPDAC	Polypoid obstruction; carcinoma *in situ*	Normal

NOTE: Only highest grade lesions observed in each mouse are listed.
Abbreviations: PA, pancreas; DU, duodenum; ST, stomach; Y, yes; N, no; IPMN-like, lesions resembling human gastric type IPMN; N/A, not available.
*Defined by >5% weight loss between 3-wk intervals where weight was examined.
†Relative percentage of abnormal structure (mPanIN, neoplasia, proliferative stroma) to the whole pancreas.

analysis showed that p15^{Ink4B} was expressed at relatively high levels in Smad4-deficient cell lines as compared with the line derived from a *Pdx1-Cre;Kras$^{G12D/+}$* animal, which indicates that other factors can maintain p15^{Ink4B} expression in the absence of Smad4 within the ductal epithelium.

***Pdx1-Cre;Kras^{G12D};Smad4$^{lox/lox}$* mice exhibit squamous cell carcinoma in the esophagus/stomach and polypoid lesion formation in the duodenum.** One limitation of the *Pdx1-Cre* transgenic system is expression of Pdx1 in regions outside of the pancreas during embryogenesis, including cells that give rise to the antral stomach and rostral duodenum (34). Although we noted no gross abnormalities in the pancreas of *Pdx1-Cre;Smad4$^{lox/lox}$* mice up to 6 months of age, all *Pdx1-Cre;Smad4$^{lox/lox}$* mice examined (n = 10) displayed significant polyp formation and had occasional cellular atypia in the duodenum that was not observed in age-matched *Pdx1-Cre* control or in *Pdx1-Cre;Kras$^{G12D/+}$* animals (Fig. 5, compare *A* and *B* with *C* and *D*). Polyps in *Pdx1-Cre;Smad4$^{lox/lox}$* mice seemed to cause moderate obstruction and occupied as much as 50% to 70% of the intestinal lumen. This level of obstruction was not severe enough to cause significant weight loss in any of the *Pdx1-Cre;Smad4$^{lox/lox}$* mice that were examined up to 14 months of age (data not shown). Cells lining the duodenum of age-matched *Pdx1-Cre;Kras$^{G12D/+}$* animals (n = 5) were mildly hyperplastic and showed cystic changes compared

with control animals (Fig. 5*B* and data not shown). Hyperplastic mucosae in the duodenum of *Pdx1-Cre;Kras*$^{G12D/+}$ animals were previously noted by others (13). In *Pdx1-Cre;Kras*$^{G12D/+}$;*Smad4*$^{lox/lox}$ mice, more pronounced neoplastic polypoid lesions were present in the duodenum along with evidence of carcinoma *in situ* by 15 weeks of age (Table 1, Fig. 5*E* and *F*). Gross examination frequently showed an enlarged duodenum (Fig. 5*G, arrow*) along with expansion of pancreatic tissue (*asterisk*).

Analysis of the stomach and esophagus in moribund *Pdx1-Cre;Kras*$^{G12D/+}$;*Smad4*$^{lox/lox}$ mice showed that 4 of 16 animals had squamous cell carcinoma that arose either from the stomach or from the esophagus as early as 6 weeks of age (Table 1; Fig. 5*K–M*). In two instances, carcinoma was noted to extend into the muscularis propria of the esophagus (Table 1, mouse nos. 62 and 490). Analysis of *Pdx1-Cre;Kras*$^{G12D/+}$ mice (n = 5) showed more subtle polypoid and hyperplastic foveolar cell changes in both the stomach and esophagus (Fig. 5*I* and data not shown). Characterization of *Pdx1-Cre;Smad4*$^{lox/lox}$ animals at 30 weeks of age revealed polypoid lesions in the stomach of two of four animals (Fig. 5*J*). The abnormal changes associated with the stomach/esophagus in *Pdx1-Cre;Smad4*$^{lox/lox}$ animals did not result in any death in animals observed beyond 14 months of age (n = 8). The complex phenotypes arising in moribund *Pdx1-Cre;Kras*$^{G12D/+}$;*Smad4*$^{lox/lox}$ mice often made it difficult to ascertain the precise cause of death, which occurred with a mean survival of 16 weeks (n = 16; Table 1; Supplementary Fig. S6 for Kaplan-Meier survival curve). However, it was clear that more than half of all moribund *Pdx1-Cre;Kras*$^{G12D/+}$;*Smad4*$^{lox/lox}$ animals had very little normal pancreatic tissue, which would have contributed significantly to the pathology observed in the animals, and other mice clearly showed evidence of advanced carcinomas/sarcomas that in all likelihood caused the death of the animals.

Discussion

Homozygous deletions and intragenic mutations at the *SMAD4* locus on human chromosome 18q21.1 occur predominantly in pancreatic cancer and at reduced frequencies in colorectal and gastric cancers (22, 25, 43, 44). The specific association of loss of SMAD4 with defined cancer types supports the importance of TGFβ signaling in suppression of these malignancies. In PDAC, loss of SMAD4 occurs late in disease progression at a stage typically associated with invasive disease and subsequent to loss of the tumor suppressor genes, *p16*^{INK4A} and *p53*, and activating mutations in *KRAS* (23). In our studies, homozygous deletion of *Smad4* in the context of an activating *Kras*^{G12D} mutation significantly accelerated neoplastic changes in the ductal epithelium that resembled both mPanIN and IPMN of the gastric/foveolar type and promoted active fibrosis that was associated with significant acinar cell loss. These changes occurred without the loss of p53 or p16^{Ink4A} (Fig. 4). Interestingly, the loss of Smad4 only seemed to promote disease progression in the presence of the *Kras*^{G12D} mutation because we observed no abnormal pancreatic histology or illness in 23 *Pdx1-Cre;Smad4*$^{lox/lox}$ animals that were

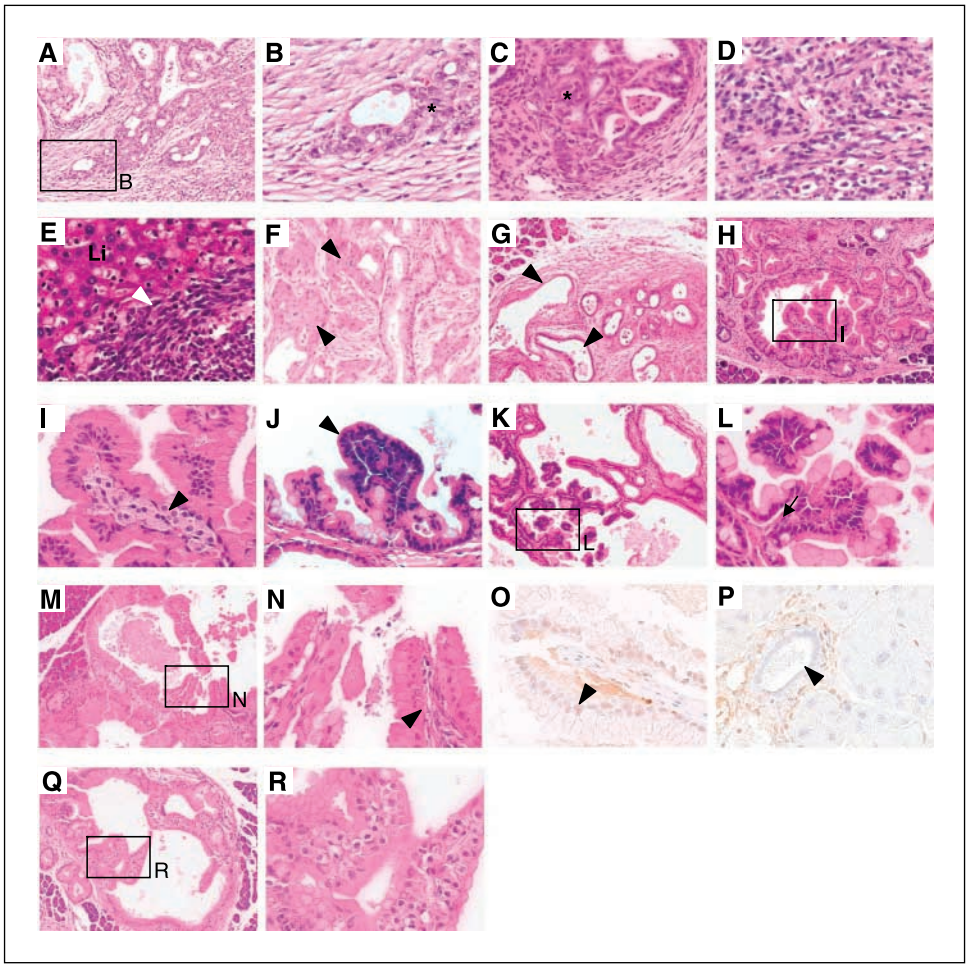

Figure 2. Invasive PDAC and other histologic features in *Pdx1-Cre;Kras*$^{G12D/+}$;*Smad4*$^{lox/lox}$ pancreas. *A* to *C,* localized development of invasive PDAC that was moderately differentiated (*asterisk*) was observed in 33-wk-old (*A* and *B*; mouse 162; ×200 and ×600) and 25-wk-old (*C*; mouse 7; ×400) *Pdx1-Cre;Kras*$^{G12D/+}$;*Smad4*$^{lox/lox}$ animals. *D* and *E,* sarcomatoid lesions in a 23-week-old double-mutant pancreas (*D*; mouse 239; ×400) that also exhibited liver metastasis (*E; white arrowhead*; ×400; *Li,* liver). *F,* adenosquamous carcinoma (*arrowheads*) in a 6-wk-old animal (mouse 484). *G,* IPMA with duct ectasia and pancreatitis (*arrowheads*) in a representative 6-wk-old *Pdx1-Cre;Kras*$^{G12D/+}$;*Smad4*$^{lox/lox}$ mouse (mouse 490; ×100). *H* and *I,* IPMN of the gastric-foveolar type showing endocrine cells within the papilla (*arrowhead*; mouse 7; ×200 and ×400). *J,* IPMN with rare papilla with acinar cells at the tip (*arrowhead*; mouse 537; ×400). *K* and *L,* IPMN involving the branch ducts with papillae formation in a 14-wk-old animal (mouse 537; ×100 and ×400). *M* and *N,* 24-wk-old *Pdx1-Cre;Kras*$^{G12D/+}$ animal with evidence of IPMN (*arrowhead*; ×100 and ×400). *O* and *P,* immunohistochemical staining showing Smad4 expression in preinvasive ductal epithelium in IPMN observed in *Pdx1-Cre;Kras*$^{G12D/+}$ animal (*O*) and the lack of Smad4 expression in a *Pdx1-Cre;Smad4*$^{lox/lox}$ control ductal epithelium (*P*; see *arrowheads*; ×400). *Q* and *R,* ductulo-insular structure present within *Pdx1-Cre;Kras*$^{G12D/+}$ mouse (×100 and ×400).

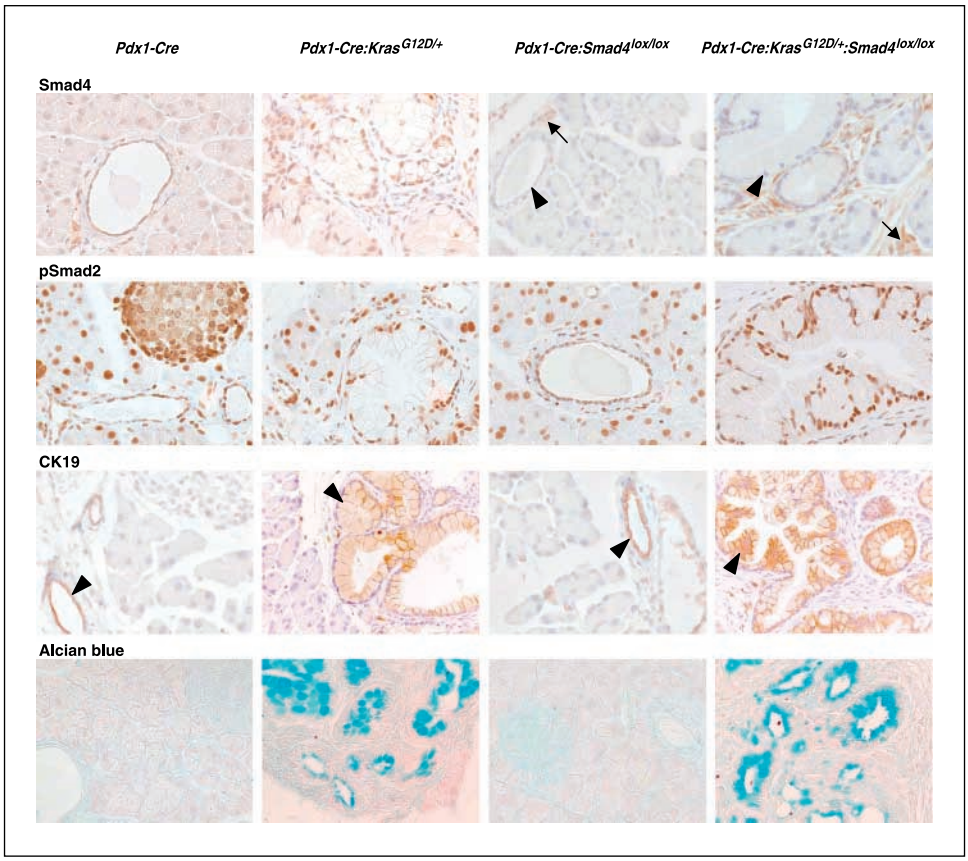

Figure 3. Immunohistochemical analysis of *Pdx1-Cre* control and mutant pancreata. *Row 1,* Smad4 expression is lacking in the ductal epithelium (*arrowheads*) in *Pdx1-Cre;Smad4$^{lox/lox}$* and *Pdx1-Cre;Kras$^{G12D/+}$;Smad4$^{lox/lox}$* mice, whereas surrounding stromal cells (*arrows*) express high levels of Smad4. *Row 2,* phospho-Smad2 staining indicating nuclear pSmad2 expression in the absence of Smad4. *Row 3,* CK19 expression indicating the epithelial phenotype of ductal lesions (*arrowheads*). *Row 4,* Alcian blue staining shows acidic mucin content within ducts. All images are at ×400.

analyzed up to 14 months of age. This indicates that Smad4 is dispensible for normal pancreatic development but is critical for at least partial suppression of multiple Kras^{G12D}-dependent disease-associated phenotypes.

Previous studies using the *Pdx1-Cre* transgenic model in mice have shown that homozygous loss of either p53 or p16^{Ink4A} in conjunction with the *Kras^{G12D}* mutation results in the development of lethal pancreatic malignancies by 8 and 18 weeks of age, respectively (21). Deletion of both p16^{Ink4A} and p19^{Arf} (in the presence of wild-type p53) accelerated lethality to 8 to 11 weeks, which indicates that both the p53 and pRb pathways are critical for suppression of PDAC progression (14, 21). In the context of *Pdx1-Cre;Kras$^{G12D/+}$;Smad4$^{lox/lox}$* mice, death occurred with a mean latency of 16 weeks, although death was likely due to tumor formation in the gastric epithelium and not to pancreatic abnormalities in ~25% of cases (Table 1). However, all moribund animals showed significant histopathologic abnormalities affecting both the pancreatic tissue and the stroma at the time of sacrifice that were substantially more progressed than age-matched *Pdx1-Cre;Kras$^{G12D/+}$* mice (Fig. 2*B* and Supplementary Fig. S1). Although *Pdx1-Cre;Kras$^{G12D/+}$;Smad4$^{lox/lox}$* mice progressed to locally invasive PDAC (Fig. 2*A–C*), their less aggressive pancreatic phenotype compared with *Pdx1-Cre;Kras^{G12D}* animals with homozygous deletions in *p53* or *p16^{Ink4A}* supports observations in human disease where these mutations (particularly loss of p16^{INK4A} expression) occur in association with SMAD4 inactivation (11). The observation that p53, p16^{Ink4A}, and p15^{Ink4B} continue to be expressed at apparently wild-type levels in ductal epithelial cell lines cultured from moribund *Pdx1-Cre;Kras$^{G12D/+}$;Smad4$^{lox/lox}$* mice might explain the less aggressive disease presentation,

Table 2. Percentage Ki-67–positive ductal cells

	Normal	mPanIN 1A	mPanIN 1B	mPanIN 2	mPanIN 3	mPDAC
Pdx1-Cre	2.2% (699)	—	—	—	—	—
Pdx1-Cre;Kras$^{G12D/+}$	5.9% (223)	10.4% (128)	24.1% (191)	69.4% (280)	—	—
Pdx1-Cre;Smad4$^{lox/lox}$	1.0% (513)	—	—	—	—	—
Pdx1-Cre;Kras$^{G12D/+}$;Smad4$^{lox/lox}$	—	16.5% (240)	31.4% (212)	81.9% (275)	90.6% (178)	92.5% (65)

NOTE: Percentage of Ki-67–positive ductal cells within preinvasive ductal lesions in mice of the defined genotypes. The total number of ductal cells counted from at least three independent mice per genotype is shown in parentheses. Statistically significant differences in the frequencies of proliferating ductal cells were noted in mPanIN-1A ducts typed from *Pdx1-Cre;Kras$^{G12D/+}$* animals versus *Pdx1-Cre;Kras$^{G12D/+}$;Smad4$^{lox/lox}$* mice ($P < 0.05$) but not at other mPanIN stages, although all stages showed a trend toward increased proliferation with loss of Smad4.

especially with respect to metastasis, as compared with $Kras^{G12D}$-expressing animals that lack p53 or $p16^{Ink4A}/p19^{Arf}$.

In contrast to previous murine studies where mPanIN was observed in association with $Kras^{G12D}$ expression, the loss of Smad4 in the context of the *Kras*^{G12D} mutation resulted in the development of preinvasive IPMN-like lesions that were evident in the majority (14 of 16) of both young and older *Pdx1-Cre;Kras*$^{G12D/+}$*;Smad4*$^{lox/lox}$ mice (Fig. 2*G–L*; Table 1). These observations contrast with human IPMN cases, which exhibit activated KRAS expression but typically not the loss of SMAD4 (32, 33). This suggests that development of IPMN may occur through distinct genetic pathways in mice as compared with humans. Alternatively, IPMN-like changes associated with Smad4 loss in mice may be occurring due to the continued presence of $p16^{Ink4A}$ and/or p53, which may be altering the normal genetic progression pathways associated with development of IPMN and mPanIN. This suggestion is supported by a recent study from the DePinho group, where they elegantly show that loss of $p16^{Ink4A}$/$p19^{Arf}$ results in a decreased incidence of IPMN in the context of either *Pdx1-Cre;Kras*$^{G12D/+}$*;Ink4a/Arf*$^{lox/lox}$*;Smad4*$^{lox/lox}$ or *Ptfa1-Cre;Kras*$^{G12D/+}$*;Ink4a/Arf*$^{lox/lox}$*;Smad4*$^{lox/lox}$ mice (45). With respect to both the subtype and incidence of IPMN and to overall survival and pancreatic histopathology, our observations of *Pdx1-Cre;Kras*$^{G12D/+}$*;Smad4* $^{lox/lox}$ mice are consistent with this recent study. Significantly, we also noted rare focal, gastric-type IPMN in two of six older *Pdx1-Cre;Kras*$^{G12D/+}$ mice that was not associated with the loss of Smad4 (Fig. 2*M–P*), although the appearance of IPMN was extremely rare in *Pdx1-Cre;Kras*$^{G12D/+}$ animals. This suggests that IPMN in mice may develop by a Smad4-independent pathway, as is presumably the case for human pancreatic tumors exhibiting IPMN. In another study, IPMN was not noted in the context of *Ptfa1-Cre;Kras*^{G12D}*;Tgfbr2*$^{lox/lox}$ mice, where rapid lethality and PDAC arise in the context of mPanIN and desmoplasia (46). The contrasting ductal phenotypes associated with $Kras^{G12D}$ expression and the loss of either Smad4 or the type II TGFβ receptor could reflect a loss of responsiveness to other receptor signaling pathways that use Smad4, like activin or BMP. Alternatively, these differences may highlight the importance of Smad4-independent pathways in rapid tumor promotion in the *Ptfa1-Cre;Kras*^{G12D}*;Tgfbr2*$^{lox/lox}$ model. Interestingly, mucinous cystic neoplasm and not IPMN was observed in another very recent study of *Ptfa1-Cre;Kras*^{G12D}*;Smad4*$^{lox/+}$ mice (47). Differences between our observations and this study could be due to modifying effects of the genetic background, which was more closely C57BL/6 in our analysis. In addition, development of mucinous cystic neoplasm may be favored over IPMN in the context of Smad4 haploinsufficiency that progresses through loss of the wild-type *Smad4* allele, whereas IPMN may develop in association with rapid and complete loss of Smad4. Because another study noted IPMN and mPanIN in the context of *Ptfa1-Cre* (45), it is unlikely that differences in cell type– or stage-specific expression of Cre from the *Pdx1* or *Ptfa1* transgene are causing this difference in neoplastic presentation. The complete absence of ovarian-type stroma and the lack of progesterone and estrogen receptor positivity, as well as the clear involvement of cystic lesions throughout the pancreas in association with the branch (and sometimes the main) pancreatic ducts (see Supplementary Fig. S1, mouse nos. 490 and 523 as examples), strongly rule out mucinous cystic neoplasm in the context of this study.

It is presently unclear what drives the significant histopathologic changes that are observed in *Pdx1-Cre;Kras*$^{G12D/+}$*;Smad4* $^{lox/lox}$ mice. One prominent feature of Smad4 loss is the marked expansion of reactive stroma and enhanced acinar cell loss that may have been due, at least in part, to acinar-to-ductal metaplasia stimulated by $Kras^{G12D}$ expression in acinar tissue, as noted in previous transgenic and knock-in models (Fig. 1*D*; refs. 13, 48, 49). However, acinar-to-ductal metaplasia occurring in *Pdx1-Cre;Kras*$^{G12D/+}$*;Smad4*$^{lox/lox}$ mice was much more focal and less pronounced than in models where $Kras^{G12D}$ was expressed using acinar-specific transgenes or Cre-deleter strains. The

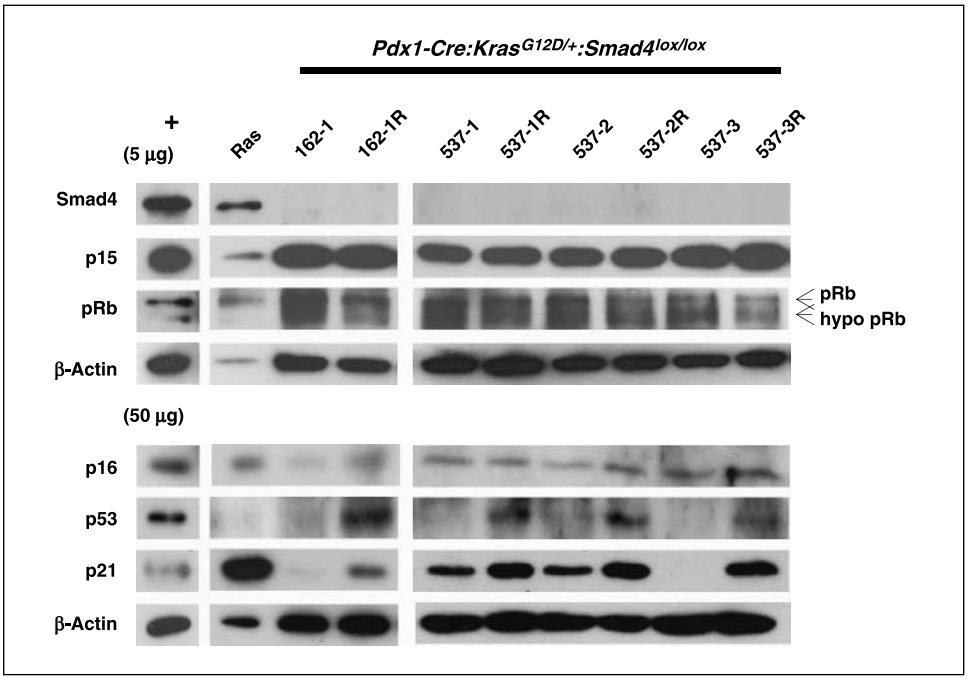

Figure 4. Western blot analysis of *Pdx1-Cre;Kras*$^{G12D/+}$*;Smad4*$^{lox/lox}$ ductal cell lines. Equivalent amounts (5 or 50 μg) of protein from a ductal cell line isolated from the pancreas of a *Pdx1-Cre;Kras*$^{G12D/+}$ mouse (*Ras*) or from independent clonal cell lines isolated from two *Pdx1-Cre;Kras*$^{G12D/+}$*;Smad4*$^{lox/lox}$ mice (mouse nos. 162 and 537) was analyzed for expression of Smad4, p15Ink4B, p16Ink4A, pRb, p53, and p21. Cell lines from *Pdx1-Cre;Kras*$^{G12D/+}$*;Smad4*$^{lox/lox}$ mice (four lines per animal, with not all lines shown) were either untreated or γ-irradiated using 10 Gy from a cobalt source (*R lanes*). *Lane* +, positive controls recommended by the antibody distributor (see Materials and Methods).

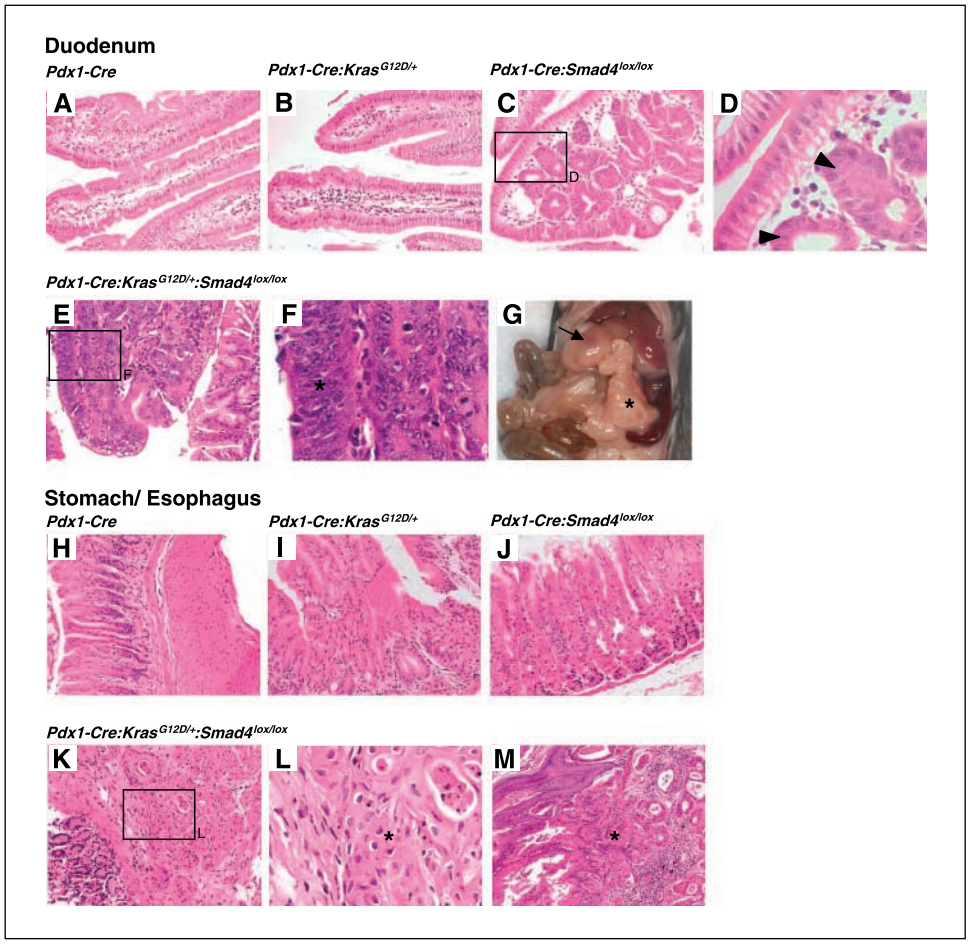

Figure 5. Effect of Smad4 inactivation on duodenum and stomach/esophagus. *A* to *F, Smad4* inactivation results in development of proliferative, mucinous crypts (*D, arrowhead*), and polypoid lesions in the duodenum of both *Pdx1-Cre;Smad4$^{lox/lox}$* and *Pdx1-Cre;Kras$^{G12D/+}$;Smad4$^{lox/lox}$* mice (age of representative mice: *A*, 33 wks; *B*, 30 wks; *C* and *D*, 33 wks; *E* and *F*, 33 wks). Carcinoma *in situ* (*F, asterisk*) was only observed in *Pdx1-Cre;Kras$^{G12D/+}$;Smad4$^{lox/lox}$* mice (*A–C* and *E*, ×200; *D* and *F*, ×600). *G,* gross anatomy of a 33-wk-old *Pdx1-Cre;Kras$^{G12D/+}$;Smad4$^{lox/lox}$* mouse illustrates significantly enlarged duodenum (*arrow*) and pancreas (*asterisk*). *H* to *J,* relatively normal stomach architecture observed in *Pdx1-Cre* control, *Pdx1-Cre;Kras$^{G12D/+}$*, and *Pdx1-Cre;Smad4$^{lox/lox}$* mice at 30 wks of age (×200). *K* and *L,* squamous cell carcinoma (*L, asterisk*) in 12-wk-old *Pdx1-Cre;Kras$^{G12D/+}$;Smad4$^{lox/lox}$* esophagus and stomach (*K*, ×200; *L*, ×600). *M,* squamous cell carcinoma (*asterisk*) in the esophagus of an 18-wk-old *Pdx1-Cre;Kras$^{G12D/+}$;Smad4$^{lox/lox}$* animal invading into the muscular parenchyma (×100).

acceleration of active fibrosis in *Pdx1-Cre;Kras$^{G12D/+}$;Smad4$^{lox/lox}$* mice could be due to enhanced expression of TGFβ1, which was noted in *Kras^{G12D};Tgfbr2* mutant mice and also in human PDAC samples (46, 50). The *Pdx1-Cre;Kras$^{G12D/+}$;Smad4$^{lox/lox}$* model may be particularly useful for future studies characterizing the role of the stromal compartment in tumor promotion and progression.

Acknowledgments

Received 11/13/2006; revised 5/1/2007; accepted 6/12/2007.

Grant support: University of Alabama at Birmingham Pancreatic Specialized Program of Research Excellence grant P20 CA101955 and a Shiota Memorial Fellowship award (K. Kojima).

The costs of publication of this article were defrayed in part by the payment of page charges. This article must therefore be hereby marked *advertisement* in accordance with 18 U.S.C. Section 1734 solely to indicate this fact.

We thank Doug Melton (Department of Molecular and Cellular Biology, Harvard University, Cambridge, MA) and Charles Murtaugh (Department of Human Genetics, University of Utah, Salt Lake City, UT) for kindly providing the Pdx1-Cre mice, Tyler Jacks (Center for Cancer Research, Massachusetts Institute of Technology, Cambridge, MA) and David Tuveson (Cancer Research UK, Cambridge Research Institute, Cambridge, United Kingdom) for the LSL-Kras^{G12D} strain, and Chu-Xia Deng (Genetics and Development and Disease Branch, National Institute of Diabetes & Digestive & Kidney Diseases, Bethesda, MD) for Smad4$^{flox/flox}$ mice; C. Rob Stockard and Jana Frost at the University of Alabama at Birmingham Tissue Procurement Core Facility for their technical help; Hideaki Ijichi and Hal Moses for sharing a protocol for primary cell line establishment; Robert Flynn, Lisa Curtis, and other members of the Klug laboratory for their insights and assistance, as well as Drs. Albert LoBuglio and Donald Buchsbaum for support.

References

1. Warshaw AL, Fernandez-del Castillo C. Pancreatic carcinoma. N Engl J Med 1992;326:455–65.
2. Jemal A, Murray T, Ward E, et al. Cancer statistics, 2005. CA Cancer J Clin 2005;55:10–30.
3. Hruban RH, Goggins M, Parsons J, Kern SE. Progression model for pancreatic cancer. Clin Cancer Res 2000; 6:2969–72.
4. Hruban RH, Wilentz RE, Kern SE. Genetic progression in the pancreatic ducts. Am J Pathol 2000;156:1821–5.
5. Hruban RH, Adsay NV, Albores-Saavedra J, et al. Pancreatic intraepithelial neoplasia: a new nomenclature and classification system for pancreatic duct lesions. Am J Surg Pathol 2001;25:579–86.
6. Hruban RH, Takaori K, Klimstra DS, et al. An illustrated consensus on the classification of pancreatic intraepithelial neoplasia and intraductal papillary mucinous neoplasms. Am J Surg Pathol 2004;28: 977–87.
7. Hezel AF, Kimmelman AC, Stanger BZ, Bardeesy N, Depinho RA. Genetics and biology of pancreatic ductal adenocarcinoma. Genes Dev 2006;20:1218–49.
8. Almoguera C, Shibata D, Forrester K, Martin J, Arnheim N, Perucho M. Most human carcinomas of the exocrine pancreas contain mutant c-K-ras genes. Cell 1988;53:549–54.
9. Klimstra DS, Longnecker DS. K-ras mutations in pancreatic ductal proliferative lesions. Am J Pathol 1994;145:1547–50.
10. Tada M, Ohashi M, Shiratori Y, et al. Analysis of K-ras gene mutation in hyperplastic duct cells of the pancreas without pancreatic disease. Gastroenterology 1996;110: 227–31.
11. Rozenblum E, Schutte M, Goggins M, et al. Tumor-suppressive pathways in pancreatic carcinoma. Cancer Res 1997;57:1731–4.
12. Moskaluk CA, Hruban RH, Kern SE. p16 and K-ras gene mutations in the intraductal precursors of human pancreatic adenocarcinoma. Cancer Res 1997;57:2140–3.
13. Hingorani SR, Petricoin EF, Maitra A, et al. Preinvasive and invasive ductal pancreatic cancer and its early detection in the mouse. Cancer Cell 2003;4:437–50.
14. Aguirre AJ, Bardeesy N, Sinha M, et al. Activated Kras and Ink4a/Arf deficiency cooperate to produce metastatic pancreatic ductal adenocarcinoma. Genes Dev 2003;17:3112–26.
15. Hruban RH, Adsay NV, Albores-Saavedra J, et al.

Pathology of genetically engineered mouse models of pancreatic exocrine cancer: consensus report and recommendations. Cancer Res 2006;66:95–106.
16. Caldas C, Hahn SA, da Costa LT, et al. Frequent somatic mutations and homozygous deletions of the p16 (MTS1) gene in pancreatic adenocarcinoma. Nat Genet 1994;8:27–32.
17. Schutte M, Hruban RH, Geradts J, et al. Abrogation of the Rb/p16 tumor-suppressive pathway in virtually all pancreatic carcinomas. Cancer Res 1997;57:3126–30.
18. Wilentz RE, Geradts J, Maynard R, et al. Inactivation of the p16 (INK4A) tumor-suppressor gene in pancreatic duct lesions: loss of intranuclear expression. Cancer Res 1998;58:4740–4.
19. Hustinx SR, Leoni LM, Yeo CJ, et al. Concordant loss of MTAP and p16/CDKN2A expression in pancreatic intraepithelial neoplasia: evidence of homozygous deletion in a noninvasive precursor lesion. Mod Pathol 2005;18:959–63.
20. Hingorani SR, Wang L, Multani AS, et al. Trp53R172H and KrasG12D cooperate to promote chromosomal instability and widely metastatic pancreatic ductal adenocarcinoma in mice. Cancer Cell 2005;7:469–83.
21. Bardeesy N, Aguirre AJ, Chu GC, et al. Both p16(Ink4a) and the p19(Arf)-p53 pathway constrain progression of pancreatic adenocarcinoma in the mouse. Proc Natl Acad Sci U S A 2006;103:5947–52.
22. Hahn SA, Schutte M, Hoque AT, et al. DPC4, a candidate tumor suppressor gene at human chromosome 18q21.1. Science 1996;271:350–3.
23. Wilentz RE, Iacobuzio-Donahue CA, Argani P, et al. Loss of expression of Dpc4 in pancreatic intraepithelial neoplasia: evidence that DPC4 inactivation occurs late in neoplastic progression. Cancer Res 2000;60:2002–6.
24. Howe JR, Roth S, Ringold JC, et al. Mutations in the SMAD4/DPC4 gene in juvenile polyposis. Science 1998; 280:1086–8.
25. Thiagalingam S, Lengauer C, Leach FS, et al. Evaluation of candidate tumour suppressor genes on chromosome 18 in colorectal cancers. Nat Genet 1996; 13:343–6.
26. Xu X, Brodie SG, Yang X, et al. Haploid loss of the tumor suppressor Smad4/Dpc4 initiates gastric polyposis and cancer in mice. Oncogene 2000;19:1868–74.
27. Fink SP, Mikkola D, Willson JK, Markowitz S. TGF-β-induced nuclear localization of Smad2 and Smad3 in Smad4 null cancer cell lines. Oncogene 2003;22:1317–23.
28. Subramanian G, Schwarz RE, Higgins L, et al. Targeting endogenous transforming growth factor β receptor signaling in SMAD4-deficient human pancreatic carcinoma cells inhibits their invasive phenotype. Cancer Res 2004;64:5200–11.
29. Levy L, Hill CS. Smad4 dependency defines two classes of transforming growth factor β (TGF-β) target genes and distinguishes TGF-β-induced epithelial-mesenchymal transition from its antiproliferative and migratory responses. Mol Cell Biol 2005;25:8108–25.
30. Sessa F, Solcia E, Capella C, et al. Intraductal papillary-mucinous tumours represent a distinct group of pancreatic neoplasms: an investigation of tumour cell differentiation and K-ras, p53 and c-erbB-2 abnormalities in 26 patients. Virchows Arch 1994;425:357–67.
31. Z'Graggen K, Rivera JA, Compton CC, et al. Prevalence of activating K-ras mutations in the evolutionary stages of neoplasia in intraductal papillary mucinous tumors of the pancreas. Ann Surg 1997;226: 491–8; discussion 8-500.
32. Furukawa T, Fujisaki R, Yoshida Y, et al. Distinct progression pathways involving the dysfunction of DUSP6/MKP-3 in pancreatic intraepithelial neoplasia and intraductal papillary-mucinous neoplasms of the pancreas. Mod Pathol 2005;18:1034–42.
33. Iacobuzio-Donahue CA, Klimstra DS, Adsay NV, et al. Dpc-4 protein is expressed in virtually all human intraductal papillary mucinous neoplasms of the pancreas: comparison with conventional ductal adenocarcinomas. Am J Path 2000;157:755–61.
34. Gannon M, Herrera PL, Wright CV. Mosaic Cre-mediated recombination in pancreas using the pdx-1 enhancer/promoter. Genesis 2000;26:143–4.
35. Gu G, Dubauskaite J, Melton DA. Direct evidence for the pancreatic lineage: NGN3+ cells are islet progenitors and are distinct from duct progenitors. Development Cambridge England 2002;129:2447–57.
36. Yang X, Li C, Herrera PL, Deng CX. Generation of Smad4/Dpc4 conditional knockout mice. Genesis 2002; 32:80–1.
37. Jackson EL, Willis N, Mercer K, et al. Analysis of lung tumor initiation and progression using conditional expression of oncogenic K-ras. Genes Dev 2001;15: 3243–8.
38. Adsay NV, Merati K, Basturk O, et al. Pathologically and biologically distinct types of epithelium in intraductal papillary mucinous neoplasms: delineation of an "intestinal" pathway of carcinogenesis in the pancreas. Am J Surg Pathol 2004;28:839–48.
39. Furukawa T, Kloppel G, Volkan Adsay N, et al. Classification of types of intraductal papillary-mucinous neoplasm of the pancreas: a consensus study. Virchows Arch 2005;447:794–9.
40. Li JM, Nichols MA, Chandrasekharan S, Xiong Y, Wang XF. Transforming growth factor β activates the promoter of cyclin-dependent kinase inhibitor p15INK4B through an Sp1 consensus site. J Biol Chem 1995;270:26750–3.
41. Datto MB, Li Y, Panus JF, Howe DJ, Xiong Y, Wang XF. Transforming growth factor β induces the cyclin-dependent kinase inhibitor p21 through a p53-independent mechanism. Proc Natl Acad Sci USA 1995; 92:5545–9.
42. Peng B, Fleming JB, Breslin T, et al. Suppression of tumorigenesis and induction of p15(ink4b) by Smad4/DPC4 in human pancreatic cancer cells. Clin Cancer Res 2002;8:3628–38.
43. Schutte M, Hruban RH, Hedrick L, et al. DPC4 gene in various tumor types. Cancer Res 1996;56:2527–30.
44. Miyaki M, Kuroki T. Role of Smad4 (DPC4) inactivation in human cancer. Biochem Biophys Res Commun 2003;306:799–804.
45. Bardeesy N, Cheng KH, Berger JH, et al. Smad4 is dispensable for normal pancreas development yet critical in progression and tumor biology of pancreas cancer. Genes Dev 2006;20:3130–46.
46. Ijichi H, Chytil A, Gorska AE, et al. Aggressive pancreatic ductal adenocarcinoma in mice caused by pancreas-specific blockade of transforming growth factor-β signaling in cooperation with active Kras expression. Genes Dev 2006;20:3147–60.
47. Izeradjene K, Combs C, Best M, et al. KrasG12D and Smad4/Dpc4 haploinsufficiency cooperate to induce mucinous cystic neoplasms and invasive adenocarcinoma of the pancreas. Cancer Cell 2007;11:229–43.
48. Grippo PJ, Nowlin PS, Demeure MJ, Longnecker DS, Sandgren EP. Preinvasive pancreatic neoplasia of ductal phenotype induced by acinar cell targeting of mutant Kras in transgenic mice. Cancer Res 2003;63:2016–9.
49. Tuveson DA, Zhu L, Gopinathan A, et al. Mist1-12D knock-in mice develop mixed differentiation metastatic exocrine pancreatic carcinoma and hepatocellular carcinoma. Cancer Res 2006;66:242–7.
50. Friess H, Yamanaka Y, Buchler M, et al. Enhanced expression of transforming growth factor β isoforms in pancreatic cancer correlates with decreased survival. Gastroenterology 1993;105:1846–56.

Inactivation of Smad4 Accelerates Kras^{G12D}-Mediated Pancreatic Neoplasia

Kyoko Kojima, Selwyn M. Vickers, N. Volkan Adsay, et al.

Cancer Res 2007;67:8121-8130.